Risk-averse Stochastic Nonlinear Model Predictive Control for Real-time Safety-critical Systems

Seyed Amin Sajadi-Alamdari * **Holger Voos** *
Mohamed Darouach **

* *Interdisciplinary Centre for Security, Reliability and Trust (SnT), University of Luxembourg, L-1359 Luxembourg, (e-mail: {amin.sajadi, holger.voos}@uni.lu)*
** *Centre de Recherche en Automatique de Nancy (CRAN) UMR-CNRS 7039, Université de Lorraine, IUT de Longwy, F-54400 Cosnes et Romain, France (e-mail: mohamed.darouach@univ-lorraine.fr)*

Abstract: Stochastic nonlinear model predictive control has been developed to systematically find an optimal decision with the aim of performance improvement in dynamical systems that involve uncertainties. However, most of the current methods are risk-neutral for safety-critical systems and depend on computationally expensive algorithms. This paper investigates on the risk-averse optimal stochastic nonlinear control subject to real-time safety-critical systems. In order to achieve a computationally tractable design and integrate knowledge about the uncertainties, bounded trajectories generated to quantify the uncertainties. The proposed controller considers these scenarios in a risk-sensitive manner. A certainty equivalent nonlinear model predictive control based on minimum principle is reformulated to optimise nominal cost and expected value of future recourse actions. The capability of proposed method in terms of states regulations, constraints fulfilment, and real-time implementation is demonstrated for a semi-autonomous ecological advanced driver assistance system specified for battery electric vehicles. This system plans for a safe and energy-efficient cruising velocity profile autonomously.

Keywords: Risk Assessment; Optimal Stochastic Control; Real-time Systems; Nonlinear and Optimal Automotive Control; Intelligent Driver Aids

1. INTRODUCTION

Model Predictive Control (MPC) has been an attractive approach for complex optimal control problems (Mayne, 2016). In the MPC, a constrained discrete-time Optimal Control Problem (OCP) is solved repeatedly in a receding horizon manner and the first control input in a finite sequence of control actions is applied to the system.

Uncertainty is a ubiquitous feature of complex dynamical systems, therefore, Robust MPC (RMPC) has been effectively utilised for systems with uncertainties (see e.g., Rawlings and Mayne (2012)). In addition to recently advanced formulations, early RMPC mainly was based on min-max OCP formulations. In many practical applications, however, worst-case based design may lead to conservative control actions and can result in low system performance. Stochastic MPC (SMPC) has been introduced to address the shortcomings of RMPC (see e.g., Bichi et al. (2010); Mayne (2016)). The SMPC is based on the stochastic uncertainty of a process model and generally expected value of the objective function with probabilistic constraints (chance-constraints) is optimised (Mesbah et al., 2014). Furthermore, Nonlinear MPC (NMPC) is distinguished by the use of nonlinear system models for prediction in order to improve performance specifications. Stochastic NMPC (SNMPC) utilises probabilistic descriptions of uncertainties such as parametric uncertainties, uncertain initial conditions, and exogenous disturbances to deal with the stochastic nonlinear systems (see e.g., Mesbah et al. (2014)).

While mostly there is no exact solution to the SNMPC problems. Several approximations have been developed to obtain a feasible solution rather than an exact solution (see e.g., Kantas et al. (2009)). Although these may not provide the optimal control performance, it make the SNMPC tractable in practice. Several works of literature about risk-neutral SNMPC have been developed (see e.g., Mesbah et al. (2014)). The main drawback of the SMPC is the risk-neutral expectation assessment of future random outcomes. This may not be a proper control policy for safety-critical systems where one desires to regulate the control actions robust enough to uncertainties (Yang and Maciejowski, 2015). Risk-sensitive control law of finite time for linear systems have been formulated (see e.g., Ito et al. (2015); Yang and Maciejowski (2015)). On the other hand, most of the SNMPCs depend on computationally expensive algorithms and few approaches have been devel-

⋆ This research was supported by FNR "Fonds national de la Recherche" (Luxembourg) through AFR "Aides à la Formation-Recherche" Ph.D. grant scheme No. 7041503.

oped about risk-averse SNMPC (see e.g., Ma et al. (2012)), as well as real-time capable SNMPC (see e.g., Ohtsuka (2004); Ohsumi and Ohtsuka (2011)).

The main contribution of this paper is a real-time risk-averse SNMPC to enhance a safety-critical Advanced Driver Assistance System (ADAS) for Battery Electric Vehicles (BEV). First, the risk-sensitive Stochastic OCP (SOCP) is adapted by a log-expectation of the exponentiated quadratic performance index. Second, in contrast to RMPC which plan for the worse case, an individual expected trajectory (scenario) is generated by a physical-statistical model of uncertainty to achieve a computationally tractable design. This helps to integrate knowledge about the disturbances and propagate the uncertainty in a bounded set. Next, the risk-sensitive SOCP is converted into a certainty equivalent OCP based on the minimum principle where the scenario is considered in a risk-averse manner. The obtained approximately equivalent problem leads to a two-point boundary-value problem based on a continuation method that can be solved in real-time. The main idea of proposed method emphasises on early detection and reduction of large recourse, rather than the compensation of non-optimal decisions. Finally, the proposed approach is evaluated in terms of states regulation, constraints fulfilment, and real-time capability for a BEV specific Semi-autonomous Ecological ADAS (SEADAS). A speed prediction model based on traffic and road geometric information is utilised to estimate an expected optimistic scenario and determines probabilist velocity profile of preceding vehicle in traffic. It is shown that the proposed system is capable of improving the safety and efficiency of the BEVs that are enduring limited cruising range.

The rest of this paper is organised as follows: The risk-averse SNMPC, uncertainty quantification, and real-time algorithm for approximated SNMPC are reviewed in section 2. The concept of the SEADAS for the BEVs with risk-averse SNMPC formulation are introduced in section 3, followed by numerical evaluations in section 4. Conclusions and future research are given in section 5.

2. STOCHASTIC PREDICTIVE CONTROL

A general nonlinear system to be controlled with disturbance is described by:

$$\dot{x} = f(x, u, \omega), \tag{1}$$
$$z = h(x), \tag{2}$$
$$\omega = \Delta(z(\cdot)), \tag{3}$$

where $x \in \mathbb{R}^{n_x}$ denotes the state vector, $u \in \mathbb{R}^{n_u}$ represents the input vector, $z \in \mathbb{R}^{n_s}$ refers to the output vector, and disturbance, $\omega \in \mathbb{R}^{n_\omega}$ is random variable vector. The $\Delta(\cdot)$ is an operator standing for unmodelled dynamics that maps the output sequence over the interval $(-\infty, t]$ into ω (Mayne, 2016).

A general multi-stage SNMPC program has the form:

$$\underset{\mu}{\text{minimise}} \quad J_N(x_t, \boldsymbol{\mu}) := \mathbf{E}[\phi(x_N^*(t)) + \sum_{i=0}^{N-1} \mathcal{L}(x_i^*(t), u_i^*(t))\Delta\tau(t)] \tag{4a}$$

$$\text{subject to:} \quad x_{i+1}^*(t) = x_i^*(t) + f(x_i^*(t), \mu_i^*(t), \omega_i(t))\Delta\tau(t), \tag{4b}$$
$$\mathbf{Pr}[h_j(x_i^*(t)) \leq 0] \geq \beta, \quad j = 1, \ldots, q, \tag{4c}$$
$$x_0^*(t) = x(t), \quad x_i^*(t) \in \mathcal{C}, \quad x_N^*(t) \in \mathcal{C}_N, \quad \boldsymbol{\mu} \in \mathcal{U}, \tag{4d}$$

where $\mathbf{E}[\cdot]$ is the mathematical expectation and $x_i^*(t)$ denotes the state vector trajectory along the prediction τ axis. The $\boldsymbol{\mu} := \{\mu_0(\cdot), \mu_1(\cdot), \ldots, \mu_{N-1}(\cdot)\}$ is an N-stage feedback control policy, which control input $u_i = \mu_i(\cdot)$ is selected at the ith stage. The $\mathcal{L} : \mathbb{R}^{n_x} \times \mathbb{R}^{n_u} \to \mathbb{R}_+$, and $\phi : \mathbb{R}^{n_x} \to \mathbb{R}_+$ are the cost-per-stage and the terminal cost functions, respectively. The $\mathbf{Pr}$ denotes probability and $h_j : \mathbb{R}^{n_x} \to \mathbb{R}$ is inequality constraint functions. The $\beta \in (0, 1) \subset \mathbb{R}$ denotes the confidence level (e.g., 0.9, 0.95, or 0.99), lower bound for probability $h_j(\cdot) \leq 0$ that should be satisfied and q is the total number of inequity constraints. The $\mathcal{C}$ is the states constraint, and $\mathcal{C}_N$ is the terminal constraint sets. The $\omega_i(t) \in \mathbb{R}^{n_\omega}$ are composed i.i.d. random variables within a sample space Ω, a set of events (σ-algebra) $\mathcal{F}$, and $\mathcal{P}$ which is the allocations of probabilities to the events (exogenous information). The $\mathcal{U} \subset \mathbb{R}^{n_u}$ denotes the set of input constraints (for more details see Mesbah et al. (2014)). The prediction horizon, T, is divided into N steps where $\Delta\tau(t) := T(t)/N$. Given the initial state, $x_0^*(t) = x(t)$, the finite sequence of control policy, $\{\mu_i^*(t)\}_{i=0}^{N-1}$, is optimized at each sampling interval and the first control policy, $\mu_0(t)$, is applied to the system.

2.1 Uncertainty Quantification

Incorporating information about the uncertainty in parameters and variables can support in quantifying the uncertainty used in SOCP. The sources of uncertainty in various context emerge in mathematical models and experimental measurements such as parameter uncertainty, structural uncertainty, experimental uncertainty, and etc. Major uncertainty quantification problems deal with various uncertainty propagation methods such as Monte Carlo methods (Kantas et al., 2009), polynomial chaos expansion (Mesbah et al., 2014), Bayesian approaches (Yang and Maciejowski, 2015), etc. In addition, SOCP (4) mainly considered in various dynamic programming approaches such as Markov chain decision processes. Assuming Markovian structure, the emphasis generally is in identifying finite state and action sets. However, as the prediction horizon length increases in SNMPC and due to the increased number of possible scenarios with large state spaces, Markov approaches can lead to being a computationally expensive method (see e.g., Bichi et al. (2010)). Moreover, it is known that the prediction quality of these methods worsens within prediction horizon (see e.g., Mesbah et al. (2014); Schmied et al. (2015)).

Different models generally have various evaluation costs and fidelities, where high-fidelity models are usually more accurate but computationally expensive than the low-fidelity models. For practical applications, it is a reasonable approach to replace every random variable by their expected values, which lead to a more simple certainty equivalent NMPC (so-called expected value problem), or several deterministic programs, where each solution is corresponded to one particular scenario (see e.g., Ohsumi and Ohtsuka (2011)). Typically, scenarios can be obtained based on information over the random variables comes from historical data (Birge and Louveaux, 2011). The two classical reference scenarios are the expected value of the random variable and the worst-case scenario. In this paper, however, to refine the bounds on the random variable vector in SNMPC, a dynamic optimistic scenario

is proposed to forward propagating the random variable vector along the prediction horizon (rolling disturbance estimation). Subject to the case study, this may be achieved by various methods such as simulation-based methods, local expansion-based methods, functional expansion-based methods, or physical-statistical models.

2.2 Risk-averse Predictive Control

Finding a solution for the SNMPC (4) that is ideal for all possible scenarios is a challenging task. Generally one may replace uncertainties with samples that can be represented as scenarios. Scenarios are based on pessimistic, neutral, or optimistic realisations of uncertainties. The OCP with expected values that represent only one scenario may be regarded as a poor representation of risk-aversion. However, the uncertain dynamic model captures one essential feature of the problem in the evolution of the scenario, which even simple models can lead to significant savings from non-optimal decisions (Birge and Louveaux, 2011). In this paper, it is proposed to propagate the system uncertainties to plausible optimistic expectations. In other words, one may expect that the value of the objective of the stochastic model will closely match the realised total optimistic expected values, and regulate system states in a risk-averse manner.

One of the interesting method to include risk during decision-making process was proposed by Whittle and Kuhn (1986). In this method the expected quadratic-cost replaced by a risk-sensitive benchmark of exponential-quadratic form (Yang and Maciejowski, 2015). A typical quadratic cost over the state is as follows:

$$\mathcal{L}_Q = (x_i^* - x_{ref})^T Q (x_i^* - x_{ref}), \tag{5}$$

where Q is weighting matrix. The conventional (risk-neutral) criterion is that one chooses a policy μ to minimize $\mathbf{E}_\mu[\mathcal{L}_Q]$. This can be minimised based on the extremal principle prescribed by the Risk-Sensitive Certainty Equivalence Principle (RSCEP) with modified benchmark as follows (Whittle and Kuhn, 1986):

$$\mathcal{L}_\mu(\gamma) = -\frac{2}{\gamma}\log(\mathbf{E}_\mu[\exp(-\frac{1}{2}\gamma\mathcal{L}_Q)]), \tag{6}$$

where γ is a real scalar so-called *risk-sensitivity* parameter. This parameter determines the control behavior towards uncertainty. The case $\gamma = 0$ corresponds to *risk-neutral*, while $\gamma > 0$ stands for *risk-seeking* attitude. This paper considers the case $\gamma < 0$ that implies *risk-aversion* reaction for safety-critical systems. The expectation value in the (6) can be computed approximately by Taylor expansion as follows:

$$\mathbf{E}_\mu[\exp(-\frac{1}{2}\gamma\mathcal{L}_Q)] \approx \exp(-\frac{1}{2}\gamma\bar{\mathcal{L}}_Q)\det(I + \frac{\gamma^2}{2}\Sigma^2_{x_i^*}), \tag{7}$$

where $\bar{\mathcal{L}}_Q$ represents the quadratic cost with predicted (posterior) nominal values of uncertainties, and $\Sigma^2_{x_i^*}$ is the covariance matrix of a random variable x_i^*. Therefore, the uncertain expected posterior values of uncertainties treated with the risk-sensitive cost (6) can be approximated as:

$$\mathcal{L}_\mu(\gamma) \approx (\bar{\mathcal{L}}_Q - \frac{2}{\gamma}\log(\det(I + \frac{\gamma^2}{2}\Sigma^2_{x_i^*}))), \tag{8}$$

where $\det(I + \frac{\gamma^2}{2}\Sigma^2_{x_i^*})$ is the volume ellipsoid to the size of the uncertainty (Yang and Maciejowski, 2015).

2.3 Risk-Sensitive Minimum Principle

In general, a variety of approximation approaches for multi-stage SOCPs such as value function approximation, constraint relaxation and dualization, policy restriction, scenario generation, and Monte Carlo methods are available. The SOCP, (4), can be expressed in terms of the Lagrangian dual problem. The main idea behind the Lagrangian approaches is to place the multi-stage links into the objective so that repeated sub-problem optimisations are avoided in finding search directions (Birge and Louveaux, 2011). This emphasises on early detection and reduction of large recourse, rather than the compensation of non-optimal decisions.

The SNMPC with the risk-sensitive cost (6) is reformulated in a computationally efficient certainty equivalent SNMPC problem. One of the effective methods to solve the resulting SOCP problem in the receding horizon manner introduced by Ohtsuka (2004) that is based on Pontryagin's minimum principle. The obtained OCP can be solved efficiently by the Continuation and Generalized Minimal RESidual (C/GMRES) method instead of computationally costly iterative algorithms (see Ohtsuka (2004)). Appeal to the extremal principle prescribed by the RSCEP yields a symmetric equation system, indicating that the extended Hamiltonian formulation generalises naturally to the risk-sensitive case. The conjugate variable or auxiliary variables of the Hamiltonian formulation has an interpretation in terms of the predicted course of process and observation noise. The RSCEP, in fact, provides a stochastic minimum principle for which all variables have a clear interpretation and the desired measurable properties (see Whittle and Kuhn (1986)).

3. CASE STUDY: SEMI-AUTONOMOUS ECO-ACC

Advanced Driver Assistance Systems (ADAS) cooperated with Ecological (Eco) driving style assist human drivers to improve the safety and efficiency of driving. These can significantly improve the Battery Electric Vehicle (BEV) energy efficiency that is long-suffering from the limited cruising range on a single battery charge. In the recent years, various research works have been conducted in this field. Energy efficient NMPC to drive an Internal Combustion Engine (ICE) vehicle with variable traffic and signals at intersections was introduced by Kamal et al. (2013). A stochastic dynamic programming based control policy with a given road grade, and traffic speed information was established by McDonough et al. (2012). A Stochastic MPC (SMPC) with driver behaviour learning capability was introduced by Bichi et al. (2010). A Stochastic NMPC (SNMPC) with the target of emission, fuel efficient driving, and infrastructure-to-vehicle (I2V) communication was introduced by Schmied et al. (2015).

3.1 System Description

The Semi-autonomous Eco-ACC (SEDAS) is based on a concept that was proposed by Schwickart et al. (2015, 2016), and is the enhancement of an approach started by Sajadi-Alamdari et al. (2016). The SEDAS concept is presented in Fig. 1, which extends the functionalities of Adaptive Cruise Control (ACC) system. Similar to the

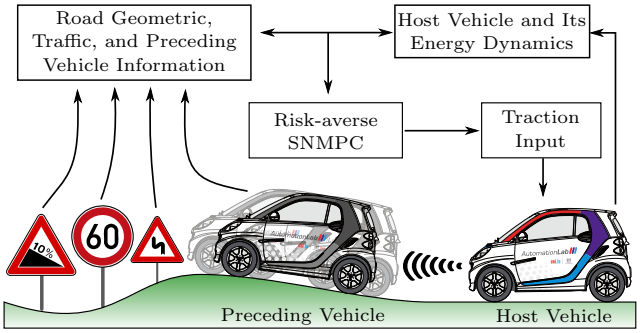

Fig. 1: Semi-autonomous Eco-ACC system (SEDAS)

conventional ACC system, the driver pre-set the desired velocity with preferred safe distance from the preceding vehicle. The Semi-autonomous Eco-ACC system regulates the traction input with respect to the longitudinal motion, energy consumption dynamics of the BEV (host vehicle), as well as the road geometric, traffic sign, and motion of the preceding vehicle information. While the driver handles the steering control of the vehicle, this system should plan for a safe and energy-efficient cruising velocity profile autonomously on the entire trip without requiring driver interventions. The longitudinal dynamics, energy consumption of the vehicle, road geometry, as well as traffic sign information, are modelled as deterministic components. The preceding vehicle's motion and its position are considered as a stochastic part of the system that imposes uncertainty during the decision-making process.

3.2 System Identifications and Models

The acceleration along the longitudinal direction of the BEV can be expressed by Newton's second law of motion as follows:

$$dv_h(t)/dt = (F_{trac}(t) - F_{res}(t))/M, \tag{9}$$

where M, $F_{trac}(t)$, and $F_{res}(t)$ are equivalent mass of the vehicle, traction force, and total motion resistive forces, respectively. The equivalent mass can be calculated by an empirical relation including kerb mass of the vehicle and equivalent mass of rotating parts (Sajadi-Alamdari et al., 2016). The traction force depends on the equivalent mass and control input as $F_{trac}(t) := Mu(t)$. The total resistive force including aerodynamic drag, gradient, and rolling resistance forces can be represented by:

$$\frac{F_{res}}{M} = \frac{1}{2M}\rho A_f C_D(d) v_h^2 + g\sin(\theta(s_h)) + C_{rr}(v_h) g\cos(\theta(s_h)), \tag{10}$$

where ρ, A_f, g, $\theta(s_h)$, and $C_{rr}(v_h)$, are the air density, the vehicle frontal area, the gravitational acceleration, the road slope angle as a function of the host vehicle position, and the velocity dependent rolling resistance coefficient, subsequently. Note that $C_D(d)$ is the aerodynamic drag coefficient that depends on nominal aerodynamic drag coefficient, and relative distance between the preceding and host vehicles, $d := s_p - s_h$. Vehicle drag reductions arising from close spacing with the preceding vehicle (for more details, see e.g. Watkins and Vino (2008)).

For any given velocity and control input, a linear relation of the traction power-to-mass ratio can describe the energy consumption of the vehicle as

$$\dot{e}_h = f_a\ (p_{trac}/M) + f_{cruise}, \tag{11}$$

where p_{trac}, denotes the traction power. The $f_a = a_2u^2 + a_1u + a_0$ and $f_{cruise} = b_3v_h^3 + b_2v_h^2 + b_1v_h + b_0$ approximate the acceleration of the vehicle and the resistive power at constant cruising velocity (Sajadi-Alamdari et al., 2016).

The road slopes, road curves, and traffic speed limit zones data are modelled as continuous and differentiable functions (Sajadi-Alamdari et al., 2016). The road slope profile is proposed to be the sum of quadratic functions of the vehicle position representing each road segments slope data as follows:

$$f_{slp}(\theta(s)) := \sum_{n=1}^{N_{sgm}} H_n(s - s_{n-1})(a_n s^2 + b_n s + c_n) H_n(s - s_n), \tag{12}$$

where N_{sgm} is the number of road segments, $H_n(s - s_{n-1})$ and $H_n(s - s_n)$ are hyper-functions of the *nth* road segment at the boundary position values, s_{n-1} and s_n. The road curves and traffic speed limits profiles are modelled based on the total absolute curve profile and the number of speed limit zones. The road curves is defined as:

$$f_{crv}(\delta(s)) := \sum_{n=1}^{N_{crv}} H_n(s - s_{ent}) \left| \frac{1}{R_{crv_n}(s)} \right| H_n(s - s_{ext}), \tag{13}$$

where N_{crv} is the number of road curves, and R_{crv_n} is the radius of a circle valid for the curve's arc length with two position points, s_{ent} and s_{ext}, at the respective entrance and exit position of the *nth* curve. The traffic speed limit places can be modelled as:

$$f_{lmt}(s) := \sum_{n=1}^{N_{lmt}} H_n(s - s_{str})(v_{lmt} - v_{max}) H_n(s - s_{end}) + v_{max}, \tag{14}$$

where N_{lmt} is the number of speed limit zones, and v_{lmt} is the specified speed limit value at positions starts from s_{str} up to the end of the zone s_{end}. The v_{max} is the maximum speed value of the vehicle (For more details see Sajadi-Alamdari et al. (2016)).

Knowledge representation of traffic including a prediction model of the plausible future motion of vehicles may improve the performance of decision-making processes in ADAS applications. Research related to anticipating the possible trajectory of the preceding vehicle into the near/far-term future has a long track in the ADAS applications. To quantify the uncertainty in the proposed concept, a physical-statistical motion model of the preceding vehicle robust to far-term future prediction is proposed in this paper. This model is based on 85^{th} percentile speed concept and road geometry information. The 85^{th} percentile speed is defined as the speed at or below which 85^{th} percent of vehicles travel a given location based on free-flowing conditions over a time period (Turne et al. (2011)). The proposed dynamic model to propagate the velocity of preceding vehicle, $\bar{v}_p$, at time t can be estimated as follows:

$$d\bar{v}_p(t)/dt := X_{85^{th}}\left(1 - \left(\frac{\bar{v}_p}{f_{85^{th}}}\right)^4 - \frac{\sin(f_{slp}(\theta(\bar{s}_p)))}{\sin(\frac{\pi}{4})}\right), \tag{15}$$

$$f_{85^{th}} := \min\{\omega_{85^{th}} v_{85^{th}}(f_{crv}(\delta(\bar{s}_p))), f_{lmt}(\bar{s}_p)\}, \tag{16}$$

$$v_{85^{th}}(\delta(\bar{s}_p)) := m_1 \exp^{(-m_2\delta(\bar{s}_p))} + m_3 \exp^{(-m_4\delta(\bar{s}_p))}, \tag{17}$$

where $X_{85^{th}}$ is the 85^{th} percentile acceleration of the preceding vehicle assumed to lie in a normal distribution i.i.d. $X \sim \mathcal{N}(\mu_p, \sigma_p)$ with the mean, μ_p, and variance σ_p^2. The $\omega_{85^{th}}$ is a tunable constant, and the position based function $v_{85^{th}}(\cdot)$, represents the 85^{th} percentile curve speed of the vehicles along the trip curves. The curve speed data is adapted from Turne et al. (2011) that can be approximated through the curve-fit process.

3.3 Problem Formulation

The risk-averse SNMPC may achieve a smarter and more energy-efficient driving based on anticipated vehicle dynamics, its energy consumption characteristics, road geometry, and traffic conditions. We interpret the position and velocity of the preceding vehicle as disturbances of the system ($\bar{\omega}_i = \mathbf{E}[\omega_i]$). The estimated disturbance concatenated as auxiliary states with the host vehicle dynamic. Thus, the states of the risk-averse SNMPC control for the proposed semi-autonomous Eco-ACC system considering the (9), (11), and (15) can be written as position, velocity, and energy consumption of the host vehicle, as well as the preceding vehicle's position and related velocity, $x = [s_h, v_h, e_h, \bar{s}_p, \bar{v}_p]^T \in \mathbb{R}^5$. Thus the (1) turns to its certainty equivalent form that the i.i.d random variable assumption is no longer required. The control input inequality constraint ($u_{min}(v_h) \leq u(t) \leq u_{max}(v_h)$) can be converted to the equality constraint by a penalty function method (Ohtsuka, 2004; Sajadi-Alamdari et al., 2016). In addition, the reference spacing policy for regulation of the safe relative distance to the preceding vehicle is based on the most commonly used method so-called *time headway*. It is defined as:

$$d_{ref} := d_0 + t_{hw} v_h, \tag{18}$$

where d_0 is a constant minimum safe distance, and t_{hw} is the desired time headway (Bayar et al., 2016).

In the risk-averse SNMPC, the following performance index to achieve the ecological driving is formulated by linearly penalising the energy consumption of the host vehicle at the end of prediction horizon as follows:

$$\phi(x_N^*(t)) := q_f e_h, \tag{19}$$

where q_f is the corresponding weight. This definition provides a flexible velocity profile planning in the integral performance index that can be formulated as follows:

$$\mathcal{L}(x_i^*(t), u_i^*(t)) := \frac{1}{2}(q_c(v_h - v_{ref})^2 + r_u(u - u_{ref})^2) - q_{slk} u_{slk} + q_{crv,lmt}(v_h, f_{crv}(\delta(s_h)), f_{lmt}(s_h)) v_h^2 + \mathcal{L}_\pi(\gamma), \tag{20}$$

where v_{ref}, u_{ref} are desired cruising velocity, and reference input respectively with relative weightings q_c, and r_u. A slack penalty, q_{slk}, is imposed to avoid the singularity at $s_{slk} = 0$ and keep the control input away from the boundary values of the feasible set. A safe and comfortable ride during the road curve and traffic speed limit zone variations can be achieved by penalising the host vehicle velocity with relative adaptive weight (similar to the barrier methods) based on the lateral acceleration ($a_{lat} = v_h^2 f_{crv}(\delta(s_h))$) and maximum allowed lateral acceleration ($a_{lat.max}$) as follows:

$$q_{crv,lmt}(v_h, f_{crv}(\delta(s_h)), f_{lmt}(s_h)) := \exp^{(q_{crv}(a_{lat} - a_{lat.max}))} + \exp^{(q_{lmt}(v_h - f_{lmt}(s_h)))}, \tag{21}$$

where q_{crv}, and q_{lmt} are relative weights.

The risk-averse cost for the relative distance implicit inequality constraint ($d_{ref} \leq d$) can be formulated as follows:

$$\mathcal{L}_\mu(\gamma) := Q_w(v_h, \bar{v}_p, d)((\mathbf{E}[d] - d_{ref})^2 - \frac{2}{\gamma}\log(1 + \frac{\gamma^2}{2}\mathbf{Var}(d))). \tag{22}$$

The statistics of the stochastic relative distance to the position of preceding vehicle can be approximated by:

$$\mathbf{E}[d] := s_p^{85^{th}} - s_h = \bar{s}_p^* - s_h^*, \tag{23}$$

$$\mathbf{Var}(d) := \mathbf{E}[(d - \mathbf{E}[d])^2] \approx \dot{d}^2 \sigma_{\bar{s}_p}^2, \tag{24}$$

where the $\mathbf{Var}[\cdot]$ is the variance of the random variable, which can be approximated by closely related moment concept in physics. The $Q_w(v_h, \bar{v}_p, d)$ is an equivalent to a soft barrier function that supplies enough weight to dominate the other objectives during close approaching to the boundary value of reference relative distance defined as follows:

$$Q_w(v_h, \bar{v}_p, d) := q_{acc}(q_{rv} \exp(\frac{-(\bar{v}_p - v_h)}{q_{rv}}) + q_{rd} \exp(\frac{\mathbf{E}[d]}{q_{rd}}))H(d_{ref} - \mathbf{E}[d]), \tag{25}$$

where q_{acc}, q_{rv}, and q_{rd} are constants, while the $H(d_{ref} - d)$ is a Heaviside's sigmoid function. The (25) can behave similarly to vanishing constraint, which smoothly switches between two modes of reference velocity tracking and ACC automatically depends on the presence of the preceding vehicle. Note that the uncertain variation position of the preceding vehicle is taken into account during decision making that allows allocation of the trade-off between risk and return of reference relative distance tracking. In other words, the presence of variance of the random variable and adaptive weights makes the controller shows proper control actions for the large system uncertainty.

4. SYSTEM EVALUATIONS

The proposed Eco-ACC system has been evaluated with practical experiments on a test track, and numerical simulations using realistic values of the parameters. A *Smart Electric Drive third generation* commercial BEV, which is available for practical experiments, is chosen here to model the dynamics of a BEV and its energy consumption (for more detail, see Sajadi-Alamdari et al. (2016)).

A closed test track located at Colmar-Berg, Luxembourg, is chosen to model the road geometry with traffic information (Fig. 2). The test track has a total length of 1.255 km and include curves, speed limit zone, and relative slope profile. This track has four main curves with 20 m, 25 m, 15 m, and 27 m radius. A speed limit zone ($v_{lmt} = 22.22\ m/s$) is assumed between positions $500 \leq s \leq 850$.

The preceding vehicle motion prediction based on 85^{th} percentile speed concept with test track geometry and speed limit zone information is shown in Fig. 3. The measured data include seven different rounds of human drivers velocity profiles on the test track. It can be shown that

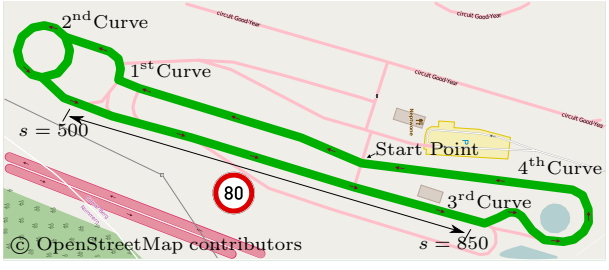

Fig. 2: Test track, Centre de Formation pour Conducteurs

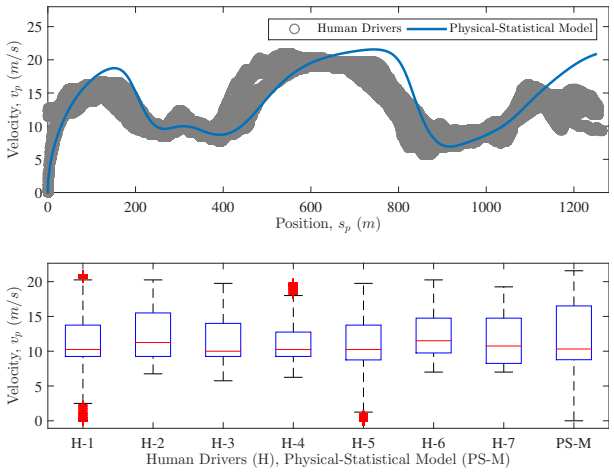

Fig. 3: A sample of far-term prediction without feedback update with relative statistics

the physical-statistical motion model is capable of foreseen an expected velocity profile based on road geometry and traffic information. Significant statistical accuracy can be shown in term of the median and the related variations from the practical experiments obtained by the human drivers (H-#), and the proposed physical-statistical motion model (PS-M) performing far-term future prediction (105 seconds) on the test track with initial state at zero without any further measurement update.

A prediction horizon for the SNMPC, $T = 15\ s$, is chosen to cover upcoming road geometry, traffic speed limit zone and the preceding vehicle motion prediction with $N = 30$ discretized steps. The constants in performance index function are set as $q_f = 2$, $v_{ref} = 20\ m/s$, $q_c = 2$, $q_{slk} = 1$, $q_{crv,lmt} = 1$, $a_{lat.max} = 3.7\ m/s^2$, $d_0 = 3\ m$, $t_{hw} = 1.5\ s$, $\gamma = -1$. The parameters for the physical-statistical model are set as $\mu_p = 0\ m/s^2$, $\delta_p = 1.5$, $\omega_{85^{th}} = 0.67$, $m_1 = 20.41$, $m_2 = 13.68$, $m_3 = 13.23$, $m_4 = 151.2$.

For the sake of comparison, the proposed risk-averse SNMPC for the Eco-ACC system is compared with a conventional nominal Deterministic NMPC (DNMPC), where a typical quadratic cost over the relative distance regulation is utilised. Furthermore, these two approach is compared with the case that the motion of the preceding vehicle is known in advance namely Perfect NMPC (PNMPC). A trigonometric speed profile for the preceding vehicle is considered as the simulation scenario to demonstrate the capabilities of the controllers in state regulations, constraint fulfilment, and energy efficiency with their treatments to unpredicted preceding vehicle speed profile.

Fig. 4. shows the obtained results by the DNMPC, SNMPC, and PNMPC for the Eco-ACC system. Fig.4a shows the velocity profile of the host and preceding vehicle with DNMPC, SNMPC, and PNMPC setting. The preceding vehicle has average velocity of $10\,m/s$, and it can be observed that the velocity profile generated by the SNMPC is closer to the PNMPC rather than the DNMPC.

Fig. 4b shows the relative distance regulation between the host and the preceding vehicles. Particularly, the SNMPC fulfils the relative distance inequality constraint with less violation rather than conventional DNMPC with relatively large constraint violations from reference rela-

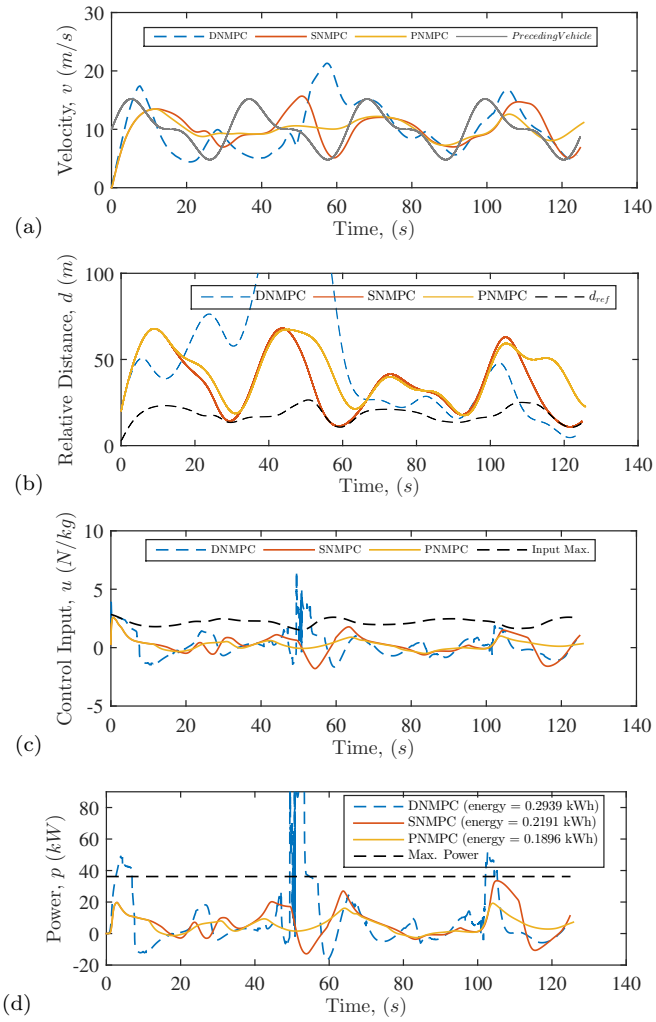

Fig. 4: Performance of the DNMPC, SNMPC, and PNMPC in terms of (a) velocity, (b) relative safe distance, (c) control input, and (d) power, with total energy consumption.

tive distance. Although the SNMPC does not know the preceding vehicle velocity profile in advance, it is shown that it can effectively regulate the safe relative distance. Fig. 4c is related to the control input profile and it is shown that the DNMPC can significantly be sensitive to unpredicted events. This leads to a non-smooth control behaviour and the maximum input constraint violation. On the other hand, the SNMPC not only demonstrates a robust behaviour against the uncertainties but also is capable of capturing similar behaviour to the PNMPC. It is shown that the SNMPC generates better velocity profile than the DNMPC, which leads to a proper energy consumption profile. This can also be observed in Fig. 4d that demonstrate the power and energy consumption of the DNMPC, SNMPC, and PNMPC with the maximum power of the host vehicle. It is shown that the DNMPC violates the maximum power constraint with higher energy consumption than the SNMPC with relatively close to the PNMPC performance.

The SOCP calculation time for the proposed SNMPC is about $3\,ms$ in average on an Intel® Core™ i7 with

memory of 7.7 GiB. The computation time of the SOCP might be compared with similar N/MPC controllers proposed in Bichi et al. (2010) with $1s$, Kamal et al. (2013) with $6.43ms$, and the Schmied et al. (2015) with $23.47ms$. Hence, the proposed SNMPC could be a real-time capable controller for the proposed Eco-ACC system.

5. CONCLUSIONS AND FUTURE RESEARCH

A real-time risk-averse stochastic nonlinear model predictive control to improve performance of safety-critical systems presented in this paper. This algorithm is based on a computationally tractable design that quantifies and integrate knowledge about the uncertainties affecting the system states. A certainty equivalent optimal control problem based on minimum principle was proposed to minimise current costs and the expected value of future recourse actions in a risk-sensitive manner. The effectiveness of the algorithm was evaluated on a semi-autonomous advanced driver assistance system for a battery electric vehicle. This system determines proper ecological velocity profile to improve safety and the cruising range based on the road geometry, traffic speed limit zones, and the preceding vehicle motion information. The key challenge in stochastic optimal control problem was to propagate the uncertainty and achieve a certainty equivalent optimal control problem, which was addressed by a physical-statistical motion model of the preceding vehicle and reformulation of the risk-averse optimal control problem. The overall performance of the proposed method reveals its capability in regulating the system states and constraints fulfilment. Extension of the proposed framework to the Connected-ACC system and further practical experiments will be conducted as the future research part.

ACKNOWLEDGEMENTS

The authors would like to acknowledge T. Schwickart, Luxembourg Fonds national de la Recherche, Delphi Automotive Systems S.A., and Centre de Formation pour Conducteurs S.A. for their valuable supports.

REFERENCES

Bayar, B., Sajadi-Alamdari, S.A., Viti, F., and Voos, H. (2016). Impact of different spacing policies for adaptive cruise control on traffic and energy consumption of electric vehicles. In *2016 24th Mediterranean Conference on Control and Automation (MED)*, 1349–1354. IEEE.

Bichi, M., Ripaccioli, G., Di Cairano, S., Bernardini, D., Bemporad, A., and Kolmanovsky, I. (2010). Stochastic model predictive control with driver behavior learning for improved powertrain control. In *49th IEEE Conference on Decision and Control (CDC)*, 6077–6082. IEEE.

Birge, J.R. and Louveaux, F. (2011). *Introduction to Stochastic Programming*. Springer Series in Operations Research and Financial Engineering. Springer New York, New York, NY.

Ito, Y., Fujimoto, K., Tadokoro, Y., and Yoshimura, T. (2015). On linear solutions to a class of risk sensitive control for linear systems with stochastic parameters. In *2015 54th IEEE Conference on Decision and Control (CDC)*, volume 4, 6516–6523. IEEE.

Kamal, M.A.S., Mukai, M., Murata, J., and Kawabe, T. (2013). Model Predictive Control of Vehicles on Urban Roads for Improved Fuel Economy. *IEEE Transactions on Control Systems Technology*, 21(3), 831–841.

Kantas, N., Maciejowski, J.M., and Lecchini-Visintini, A. (2009). Sequential Monte Carlo for Model Predictive Control. In *Nonlinear Model Predictive ...*, 263–273.

Ma, Y., Vichik, S., and Borrelli, F. (2012). Fast stochastic MPC with optimal risk allocation applied to building control systems. In *2012 IEEE 51st IEEE Conference on Decision and Control (CDC)*, 7559–7564. IEEE.

Mayne, D. (2016). Robust and stochastic model predictive control: Are we going in the right direction? *Annual Reviews in Control*, 41, 184–192.

McDonough, K., Kolmanovsky, I., Filev, D., Yanakiev, D., Szwabowski, S., and Michelini, J. (2012). Stochastic dynamic programming control policies for fuel efficient in-traffic driving. In *2012 American Control Conference (ACC)*, 734, 3986–3991. IEEE.

Mesbah, A., Streif, S., Findeisen, R., and Braatz, R.D. (2014). Stochastic nonlinear model predictive control with probabilistic constraints. In *2014 American Control Conference*, 2413–2419. IEEE.

Ohsumi, K. and Ohtsuka, T. (2011). Particle Model Predictive Control for Probability Density Functions. *IFAC Proceedings Volumes*, 44(1), 7993–7998.

Ohtsuka, T. (2004). A continuation/GMRES method for fast computation of nonlinear receding horizon control. *Automatica*, 40(4), 563–574.

Rawlings, J.B. and Mayne, D.Q. (2012). *Model Predictive Control: Theory and Design*. Nob Hill Publishing.

Sajadi-Alamdari, S.A., Voos, H., and Darouach, M. (2016). Nonlinear model predictive extended eco-cruise control for battery electric vehicles. In *2016 24th Mediterranean Conference on Control and Automation (MED)*, 467–472. IEEE, Athens.

Schmied, R., Waschl, H., Quirynen, R., Diehl, M., and del Re, L. (2015). Nonlinear MPC for Emission Efficient Cooperative Adaptive Cruise Control. *IFAC-PapersOnLine*, 48(23), 160–165.

Schwickart, T., Voos, H., Hadji-Minaglou, J.R., Darouach, M., and Rosich, A. (2015). Design and simulation of a real-time implementable energy-efficient model-predictive cruise controller for electric vehicles. *Journal of the Franklin Institute*, 352(2), 603–625.

Schwickart, T., Voos, H., Hadji-Minaglou, J.R., and Darouach, M. (2016). A Fast Model-Predictive Speed Controller for Minimised Charge Consumption of Electric Vehicles. *Asian Journal of Control*, 18(1), 133–149.

Turne, D.S., Peter M. Briglia, J., and Fitzpatrick, K. (2011). Modeling Operating Speed: Synthesis Report. Technical Report July, Washington, DC.

Watkins, S. and Vino, G. (2008). The effect of vehicle spacing on the aerodynamics of a representative car shape. *Journal of Wind Engineering and Industrial Aerodynamics*, 96(6-7), 1232–1239.

Whittle, P. and Kuhn, J. (1986). A hamiltonian formulation of risk-sensitive Linear/quadratic/gaussian control. *International Journal of Control*, 43(1), 1–12.

Yang, X. and Maciejowski, J. (2015). Risk-Sensitive Model Predictive Control with Gaussian Process Models. In *IFAC-PapersOnLine*, volume 48, 374–379. Elsevier B.V.